Inwardly rotating spiral wave breakup in oscillatory reaction-diffusion media

Fagen Xie,[1] Dongzhu Xie,[2] and James N. Weiss[3]
[1]*Research Department, Kaiser Permanente, 100 S. Los Robles Ave, Pasadena, California 91101, USA*
[2]*Department of Physics, Shanghai Normal University, Shanghai 200233, People's Republic of China*
[3]*UCLA Cardiovascular Research Laboratory, Departments of Medicine (Cardiology) and Physiology, David Geffen School of Medicine at UCLA, Los Angeles, California 90095, USA*
(Received 19 August 2005; revised manuscript received 14 March 2006; published 8 August 2006)

The breakup of inwardly rotating spiral waves has been investigated in an oscillatory reaction-diffusion system near a Hopf bifurcation point. The breakup first occurred at the region far away from the core area, then gradually involved the whole medium by increasing the diffusion coefficient ratio between the two components of the oscillator system. With the approximation of the Complex-Ginzburg-Landau equation (CGLE), the criteria for the occurrence of the inwardly rotating spiral wave are examined theoretically. The analysis of the stability in the corresponding CGLE revealed that the breakup of the inward spiral wave was related to the Eckhaus instability.

DOI: 10.1103/PhysRevE.74.026107 PACS number(s): 82.40.Ck, 05.45.−a, 47.54.−r

I. INTRODUCTION

Spiral wave dynamics has been investigated extensively in a variety of physical, chemical, and biological systems [1]. Usually, spiral waves in excitable reaction-diffusion systems rotate outwardly through the medium from the spiral core area [1]. Recently, an interesting inwardly rotating spiral wave was observed in the oscillatory Belousov-Zhabotinsky (BZ) reaction dispersed in water droplets of a water-in-oil aerosol OT (AOT) microemulsion (BZ-AOT system) [2]. The propagating direction of a spiral wave is determined by the sign of the phase velocity in the system, and the spiral propagates outwardly (inwardly) for positive (negative) phase velocity [3–6]. The transition between outward spiral and inward spirals has been investigated theoretically and numerically in various oscillatory reaction-diffusion systems, and in the corresponding complex Ginzburg-Landau equation (CGLE) [5,6].

The breakup of outwardly rotating spiral waves has been observed and studied in various systems [1,7–17]. In particular, spiral wave breakup has been hypothesized to be a mechanism of cardiac fibrillation—the leading killer in industrialized countries [16,17]. Phenomenologically, two different kinds of breakup scenarios for outward spiral waves have been documented in experimental and numerical simulations: spirals in excitable media usually break near the spiral core [7,8], while spirals in the oscillatory media first become unstable far away from the core [9–15]. The breakup near the spiral core center is related to a Doppler-induced meandering instability [7,8], while the breakup far away from the core area is caused by the absolute Eckhaus instability [9–15]. However, to our knowledge, there is no information on whether an inwardly rotating spiral wave can breakup into a turbulencelike state, and, if so, what mechanism is involved. In this paper, we focus our investigations on this problem using a FitzHugh-Nagumo (FHN)–type oscillatory system. In the next section, we present the mathematical model and the numerical simulations of inward spiral wave breakup in this system. The theoretical analysis of the inward spiral waves and breakup due to the Eckhaus instability under the approximation of CGLE is presented in Sec. III. The paper ends with the conclusions and discussion of the results.

II. MATHEMATICAL MODEL AND BREAKUP OF INWARD ROTATING SPIRAL WAVE

The oscillatory system under investigation consists of the following reaction-diffusion equations [18]:

$$\partial u/\partial t = (u - u^3/3 - v)/\varepsilon + Du\nabla^2 u,$$

$$\partial v/\partial t = u - \sigma v + \delta + Dv\nabla^2 v, \qquad (1)$$

where ε, σ, and δ are the system control parameters. D_u and D_v are the homogenous diffusion coefficients for the activator (u) and inhibitor (v), respectively. As $\varepsilon \leqslant \varepsilon_c = (1-u_0^2)/\sigma$, where, u_0 is the fixed point at ε_c, a limit cycle with a frequency $\Omega = \sqrt{\sigma/(1-u_0^2) - \sigma^2}$ in the local dynamics of Eq. (1) appears via a supercritical ($g' > 0$) Hopf bifurcation. An inwardly rotating spiral wave was numerically simulated in a two-dimensional homogeneous medium with an identical small value of diffusion coefficient for both u and v near the Hopf Bifurcation point [4]. The criteria for the occurrence of the inward rotating spiral waves and the transition between the outward spiral and inward spirals in the system have been examined in detail [4–6]. In this paper, we focused our attention on how inwardly rotating spiral waves, could breakup into a complex spatiotemporal chaos or turbulentlike state. It is well-known that new patterns, such as Turing patterns, can emerge in reaction-diffusion systems in which there is an imbalance between the diffusion coefficients D_u and D_v [19,20]. Therefore, we set $\gamma = D_v/D_u$, and investigated whether an inward spiral wave would break up into complex spatiotemporal chaos when the diffusion ratio γ was varied. Throughout this paper, we fixed $\varepsilon = 1.95$, $\sigma = 0.5$, $\delta = 0.0$, $D_u = 0.004$, and then varied γ. With $\sigma = 0.5$ and $\delta = 0.0$, the Hopf bifurcation occurred at $\varepsilon_c = 2$. Equation (1) was simulated in a two-dimensional (2D) square sheet with size $L = 100.0$. No-flux boundary conditions and dis-

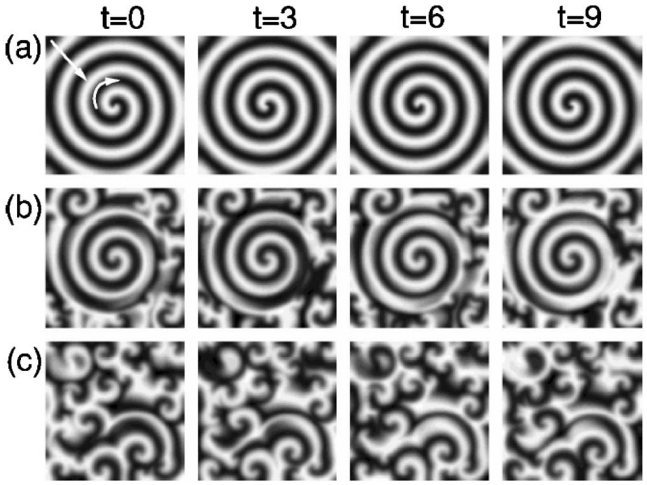

FIG. 1. Snapshots of u in the FHN model (1) at different times and γ. The black to white gray scale represents the lowest value (–0.6) to the highest value (0.6). The arrows indicate the direction of wave propagation. (a) $\gamma=1.0$; (b) $\gamma=3.5$; (c) $\gamma=4.0$.

cretization of $dx=dy=0.5$ and $dt=0.01$ were used in an explicit Euler-scheme. Since we studied the instability of a single inwardly rotating spiral wave, the spiral wave was first initiated by using the limit cycle obtained from the local dynamics of Eq. (1) for $\gamma=1$ rather than random conditions, which could initiate multiple spirals [4]. The spiral wave was then initiated with the values of previous final stable spiral by gradually increasing γ.

As the diffusion ratio γ increased from *one* (the balanced value for u and v), the dynamical behavior of the inwardly rotating spiral wave qualitatively changed. For small γ, the inward spiral wave was completely stable everywhere. The snapshots of u for $\gamma=1.0$ are shown in Fig. 1(a). The spiral wave propagated from the boundary of the medium to the spiral core center (propagation of stable inwardly rotating spiral waves can be viewed in the online supplemental in Ref. [21] [movie stable_inward_spiral.avi]). The corresponding trajectories of the spiral core center and the spiral arm (far away from the core center) and the variation of the maximized u measured for each spiral rotating period at $y=50.0$ through the spiral core center is shown in Figs. 2(a) and 2(b), respectively. The inside left-upper inset in Fig. 2(a) shows an enlargement of the trajectory at the core center ($x=50.0$, $y=50.0$). The spiral core center was not completely fixed, but oscillated with a small amplitude. The unique maximized u value for each x along the x axis demonstrates that the inward spiral wave was completely stable. However, as γ increased to a critical value $\gamma\approx3.3$, an unstable modulation developed in regions near the boundary. These oscillations eventually grew larger enough to cause the spiral arm near the boundary to break up into complex multiple inward spirals, while the core center region remained stable (a movie illustrating the dynamical evolution of the inward spiral wave can be viewed in Ref. [21] [partly_inward_spiral_breakup.avi]). Figures 1(b), 2(c), and 2(d) show the dynamical behaviors for $\gamma=3.5$. The stable part of the inward spiral wave in the core area was surrounded by a complex sea of inward spirals in Fig. 1(b). The

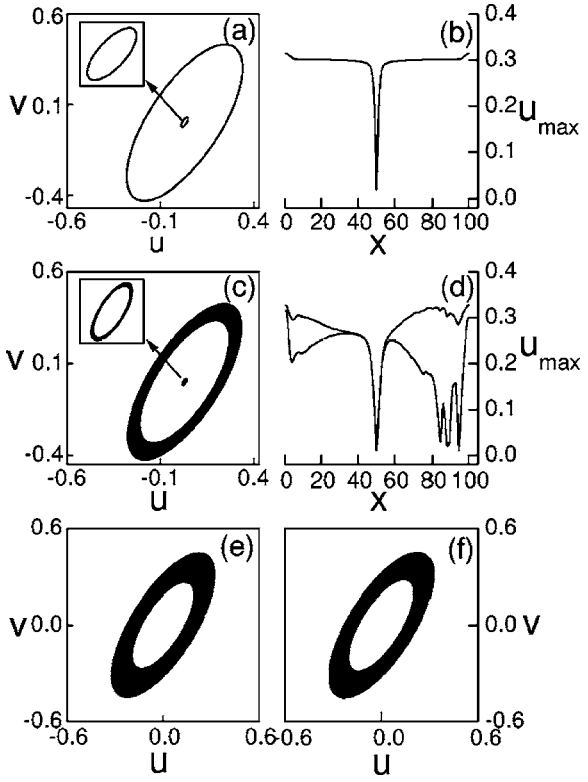

FIG. 2. The corresponding trajectories [left column and (f)] for locations $x=50.0$, $y=50.0$, and $x=85.0$, $y=50.0$, and the minimum and maximum of the maximized u measured from each rotating or oscillating period [right column, except (f)] versus x at $y=50.0$. The parameters in (a) and (b), (c) and (b), (e) and (f) were the same as those in 1(a)–1(c), respectively. The small and large oscillator or torus in (a) and (c) represents the trajectories at $x=50.0$, $y=50.0$ and $x=85.0$, $y=50.0$, respectively. The left-top part in (a) and (c) shows an enlargement of the small oscillating trajectory in the same figure. The plots in (e) show the trajectory at the center $x=50.0$, $y=50.0$ while the plots in (f) show the trajectory at the boundary location $x=85.0$ and $y=50.0$.

oscillation amplitudes of the maximized u measured from each spiral in the breakup region were of the same order [Fig. 2(d)], and the variation of the maximized u quickly decayed as the distance approached the stable core region. This phenomenon of a stable inward spiral waves surrounded by a turbulent spiral sea could be seen in the nucleation process, and was also observed for outward spiral waves in the Bar model [10]. When γ was continuously increased, the breakup gradually invaded the stable region near the core center, and finally the inward spiral wave broke up in the whole medium, as shown in Fig. 1(c) for $\gamma=4.0$ (the corresponding movie of fully developed inward spiral wave breakup can be viewed in the online supplemental in Ref. [21] [fully_inward_spiral_breakup.avi]). The irregular trajectory of the center of the medium in Fig. 2(e) was now the same as in the region near the boundary shown in Fig. 2(f). This breakup scenario is similar to the breakup of outwardly rotating spiral waves observed in numerical simulations in oscillatory diffusion-reaction systems [9–11], and experiments in BZ systems [15], which showed that spiral wave breakup in these systems was related to the Eckhaus insta-

bility, and, more importantly, the absolute instability.

It is well established that wave propagation emitted from a Dirichlet or fixed boundary in 1D systems is an approximate analog of a spiral wave in 2D medium, without the curvature effects [9–11]. The wave front or spiral arm far away from the core center could be also considered as an asymptotic plane wave [9–11]. Thus, for simplicity, we also simulated the wave dynamics of Eq. (1) in a one-dimensional cable with the Dirichlet or a fixed left boundary, and a no-flux right boundary, to explore the instability of the oscillating modulation of the inward spiral arm far away from the core center. Neglecting the small oscillation of the dynamics in the core center as shown in Fig. 2, we fixed $u(0)=v(0)=0$ at the left boundary, so this 1D fixed point was similar to the core center of the 2D inward spiral wave. Space-time plots at different times and the corresponding variation of maximum u during each wave period in 1D simulation are shown in Fig. 3 for two different γs. Although we used the fixed boundary at the left side, the wave train propagated from the right side to left side, rather than being triggered from the fixed left source point. This is consistent with inward propagation of the spiral from the boundary to the core center in 2D simulations. As shown in Figs. 3(a) and 3(b) for $\gamma=3.0$, the wave far away from the fixed boundary first displayed unstable modulated perturbation due to convective instability [9–11], but this perturbation was gradually advected to the right side, and finally disappeared. The propagated wave train exhibited an absolute instability upon increase of γ at a critical value $\gamma_c \approx 3.6$, which was little larger than the critical value of 2D inward spiral wave breakup. As $\gamma > \gamma_c$, this instability manifested itself to produce the wave train "breakup" several wavelengths from the left fixed boundary, as shown in Figs. 3(c) and 3(d) for $\gamma=3.7$.

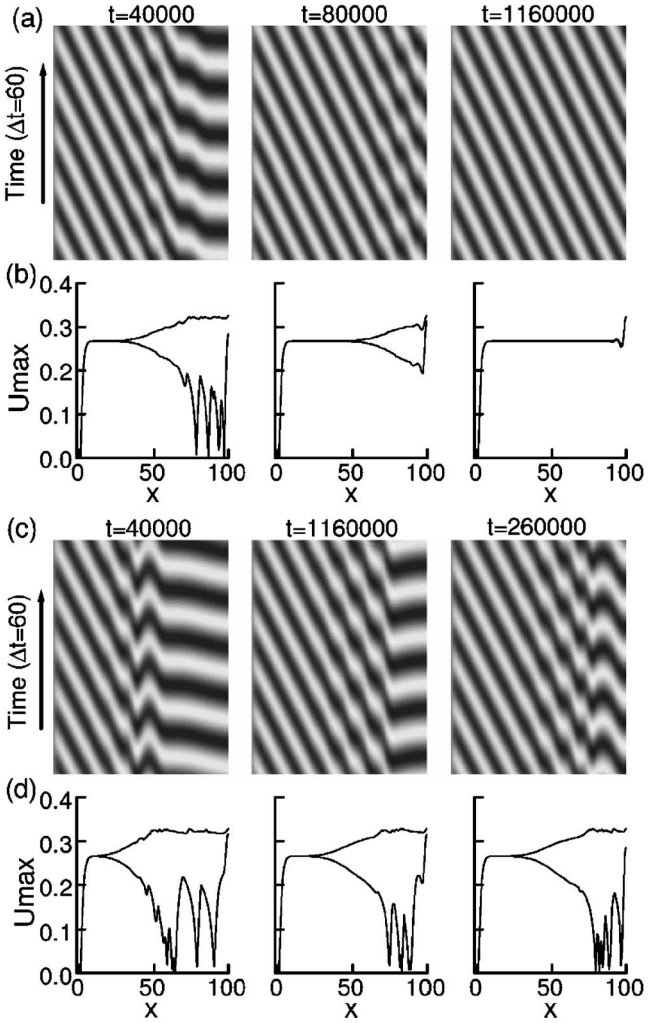

FIG. 3. Space-time plots (a) and (c) and the minimum and maximum of the maximized u during each wave propagation period within 200 000 time intervals (b) and (d) from simulations of Eq. (1) in 1D cable with left fixed and right zero-flux boundary conditions for different times and γ. (a) and (b) $\gamma=3.0$; (c) and (d) $\gamma=3.7$. The initiated disorder in (a) and (b) was finally advected away, while it manifested in (c) and (d).

III. THE STABILITY ANALYSIS OF INWARD ROTATING SPIRAL IN CGLE

The dynamics of waves in reaction-diffusion systems near a supercritical Hopf bifurcation point can be generically described by the CGLE [13,14,22]. Since the control parameter $\varepsilon=1.95$ in this paper was in the vicinity of the Hopf bifurcation point ($\varepsilon_c=2$, $\Delta\varepsilon=\varepsilon-\varepsilon_c=0.05\ll 1$), the approximation of CGLE could be considered to be valid. Using the standardized perturbation method [6,13,14,22], the following CGLE

$$\partial W/\partial t = W - (1+i\alpha)W|W|^2 + (1+i\beta)\nabla^2 W, \tag{2}$$

where

$$\alpha = g''/g' = -\sqrt{\frac{\sigma}{1-\sigma}},$$

$$\beta = d''/d' = \sqrt{\frac{\sigma}{1-\sigma}}\frac{(D_v - D_u)}{(D_v + D_u)} = \sqrt{\frac{\sigma}{1-\sigma}}\frac{(\gamma-1)}{(\gamma+1)}, \tag{3}$$

can be derived from the original reaction-diffusion system of Eq. (1) by setting $\delta=0.0$. Since we fixed $\sigma=0.5$, Eq. (3) became

$$\alpha = -1, \quad \beta = (\gamma-1)/(\gamma+1). \tag{4}$$

The spiral wave (either outwardly or inwardly) of Eq. (2) in the CGLE has the following form [6,12–14]:

$$W = F(r)\exp\{i[-\omega t - m\phi + \psi(r)]\}. \tag{5}$$

Here (r,ϕ) are the polar coordinates, $m=\pm 1$ is the topological charge of a one-arm spiral, and $\omega=\alpha+(\beta-\alpha)Q_s^2$. $F(r)$ and $\psi(r)$ are functions with the following asymptotic behavior:

$$F(0) = \psi(0) = 0, \quad \lim_{r\to\infty} F(r) = \sqrt{1-Q_s^2}, \tag{6}$$

where $Q_s=\lim_{r\to\infty}\psi'(r)$ is the asymptotic wave number which is uniquely determined by α and β [12–14,22]. ω and Q_s are antisymmetric under the transformation

$(\alpha \to -\alpha, \beta \to -\beta)$, i.e., $\omega(-\alpha,-\beta)=-\omega(\alpha,\beta)$ and $Q_s(-\alpha,-\beta)=-Q_s(\alpha,\beta)$.

Analysis of the occurrence of inward spiral wave, Asymptotically $r \to \infty$, the phase velocity v_{ph} of Eq. (2) equals to $\omega(\alpha,\beta)/Q_s(\alpha,\beta)$, where $Q_s(\alpha,\beta)$ could be calculated numerically in the 2D system [12–14,23] and analytically for the analog of a spiral in a 1D system [6]. With the parameters $\alpha=-1$, and $\beta=(\gamma-1)/(\gamma+1)>0$ in this paper, we have $\omega<0$ (spiral rotating clockwise) and $Q_s>0$, and then $v_{ph}<0$, so the spiral inwardly rotated in the CGLE. Under the approximation of CGLE, the phase velocity of spiral in the original FHN model of Eq. (1) could be simplified as $\tilde{v}_{ph} \approx -\Omega/\tilde{Q}_s \sim -\Omega/Q_s < 0$, where Ω was the frequency of the oscillator near the onset of supercritical Hopf bifurcation [6]. Therefore, the spiral in the original FHN system of Eq. (1) also inwardly rotated.

The Eckhaus instability. Equation (2) exhibits the following plane wave solutions:

$$W = F \exp\{i[Q(r-\omega t)]\}, \tag{7}$$

where $F=\sqrt{1-Q^2}$, $\omega=\alpha+(\beta-\alpha)Q^2$, and $Q^2<1$.

To analyze the stability of the plane waves, we applied a small longitudinal perturbations $\exp(\pm ikr)$ with $k \| Q$ to Eq. (7), then we obtained [see Refs. [12,13] for more details]

$$\lambda(k) = -k^2 - F^2 - 2iQ\beta k \pm \sqrt{(1+\alpha^2)F^4 - (\beta k^2 - 2iQk + \alpha F^2)^2}. \tag{8}$$

In the long-wavelength limit $(k \to 0)$, Eq. (8) can be expanded to the following formula:

$$\lambda(k) = 2i(\alpha-\beta)Qk - D_{\|}k^2 + O(k^3), \tag{9}$$

and

$$D_{\|} = 1 + \alpha\beta - 2(1+\alpha^2)Q^2/(1-Q^2). \tag{10}$$

Thus, the criteria of the long-wavelength stability of the plane waves are $D_{\|}(\alpha,\beta,Q)=0$, which are called the *Eckhaus instability*. This leads to

$$Q_c = \sqrt{\frac{1+\alpha\beta}{3+\alpha\beta+2\alpha^2}}. \tag{11}$$

So, all plane or traveling waves with $Q<Q_c$ are stable and vice versa for those with $Q>Q_c$. From Eq. (11), it is easy to obtain the result that the uniform oscillator $(Q=0)$ is the last plane wave to become unstable at the BFN boundary $1+\alpha\beta=0$. The critical wave number Q_c versus β for $\alpha=-1$ is shown in Fig. 4 by the dashed line. The area under this dashed line is the *Eckhaus stable*.

As $Q>Q_c$, the plane waves became destabilized via an Eckhaus instability. However, the instability could be convective or absolute [12,13]. For the convective instability, although the perturbations grow along space, they eventually convect away over a long time evolution. In contrast, for absolute instability, perturbations grow everywhere in the system, and the growing perturbations are not damped with any long evolution. To test the absolute instability, the following linear evolution of a small localized perturbation

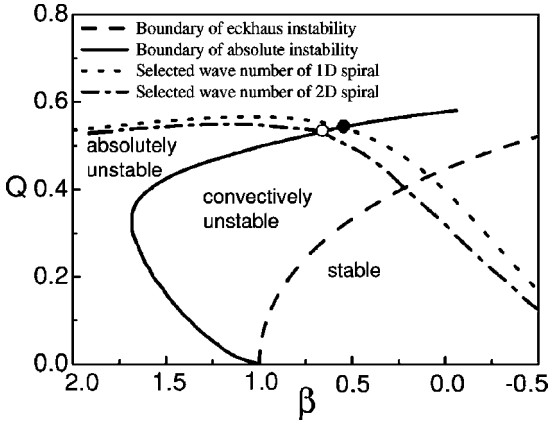

FIG. 4. The boundaries for the Eckhaus convective instability (dashed line) and absolute instability (solid line) at the Q-β plane in the CGLE of Eq. (2) for $\alpha=-1$. The dashed-dotted line and dotted line represent the wave number $Q(\beta)$ selected by the 2D inwardly rotating spiral wave and the 1D analog of a spiral in the CGLE of Eq. (2) at the limit $r \to \infty$, respectively. The open circle represents the theoretical predicted threshold of 2D inward spiral wave breakup, while the solid circle is the threshold for the 1D analog of a spiral.

$S_0(x)$ around the plane waves in the longitudinal direction $k \| Q$ has to be considered

$$S(x,t) = \frac{1}{2\pi}\int_{-\infty}^{\infty} \hat{S}_0(k)\exp[ikx + \lambda(k)t]dk, \tag{12}$$

where $\hat{S}_0(k)$ is the Fourier transformation of $S_0(x)$. The integral of Eq. (12) can be deformed into the complex k plane, and is dominated by the largest saddle point of $\lambda(k)$ [12,13]. Therefore, the criteria for the absolute instability are

$$\mathrm{Re}[\lambda(k_0)] = 0, \qquad \left.\frac{\partial\lambda}{\partial k}\right|_{k_0} = 0, \tag{13}$$

where k_0 is the largest saddle point. The threshold of Q for absolute instability determined by Eq. (13) versus β for $\alpha=-1$ is shown in Fig. 4 as the solid line. The area above the black line is *absolute unstable*, while the area between the solid and dashed lines is *convectively unstable*.

The instability of 2D spiral waves and 1D analog of spiral. Since the above Eckhaus instability analysis is independent of the phase velocity, the instability applied can be applied to either inwardly or outwardly rotating spiral waves. At the limit $r \to \infty$, the 1D analog of spiral asymptotically approaches a plane wave with the following analytical wave number [6]:

$$Q_s = -\frac{3\mu(\alpha,\beta)}{2(\beta-\alpha)} \pm \sqrt{\frac{9\mu(\alpha,\beta)^2}{4(\beta-\alpha)^2} + \frac{2\beta\mu(\alpha,\beta)^2 - \alpha}{\beta-\alpha}}, \quad \text{for } \beta-\alpha>0 \text{ and } <0, \tag{14}$$

where

$$\mu(\alpha,\beta) = \sqrt{\frac{(5+9\alpha\beta)\beta+4\alpha+3\beta\sqrt{8(\alpha+\beta)^2+9(1-\alpha\beta)^2+4\alpha\beta}}{4(2\alpha+7\beta+9\beta^3)}}.$$

The 1D analog of the spiral selected wave number obtained by Eq. (14) versus β for $\alpha=-1$ is shown in Fig. 4 with dotted lines. Thus, the threshold of instability of the 1D analog of spiral was approximately $\beta c \approx 0.55$, represented by the solid circle, the intersection point of the solid line, and the dotted line. Using the relation of Eq. (4), the analytical threshold of instability of a 1D analog of spiral in the original FHN model of Eq. (1) is $\gamma_c \approx 3.5$, which agrees well with the direct 1D numerical simulation in Fig. 3.

In the limit $r \to \infty$, the 2D spiral wave of Eq. (7) can also be asymptotic to the plane wave with $Q=Q_s$, which is uniquely determined by α and β. However, there is no theoretical analytical formula for the wave number selected by the 2D spiral wave, in general, and it must be computed numerically, as explored in details in Refs. [13,23]. The 2D spiral selected wave number obtained from numerical calculations is shown in Fig. 4 by the dashed-dotted line, which is validated from the wave number selected by the 1D analog of spiral. Therefore, the threshold of absolute instability for 2D spiral waves is the intersection of the solid line and the dashed-dotted line shown in Fig. 4 by the open circle, where $\beta c \approx 0.64$. As $\beta > \beta_c$, the spiral became unstable via the Eckhaus absolute instability, and broke up into a complex turbulencelike state. This theoretical predicted threshold was slightly larger than the critical value $\beta c \approx 0.59$ obtained by the directly numerical simulations in the CGLE of Eq. (2). The simulations for stable inward spiral and spiral wave breakup in the CGLE are shown in Fig. 5. Since the equations. of (2) and (4) are equivalent to the original reaction-diffusion system (1) under the CGLE valid approximation, the inwardly spiral wave in the original FHN model (1) also became unstable and broke up via the Eckhaus absolute instability. Using Eq. (4), the predicted threshold of inwardly spiral wave breakup in the original FHN model of Eq. (1) should be nearly $\gamma c \approx 4.5$. However, this critical value was a little different from the threshold obtained by numerical simulations in the original FHN model as shown in Fig. 1. This difference could be due to two factors. First, the spiral wave breakup occurred at a finite size (only several wavelengths from the spiral core area) in our simulations, while our theoretical analysis was based on the limit $r \to \infty$. Second, although the parameter $\varepsilon=1.95$, $\Delta\varepsilon=0.05$ was considered in the vicinity of the Hopf bifurcation point, the CGLE approximation (third order) may not be accurate enough to represent the dynamics of the original system, and higher order approximation terms need to be considered. Indeed, at $\varepsilon=1.98$ and $\Delta\varepsilon=0.02$, we numerically found that the threshold of breakup in Eq. (1) was $\gamma c \approx 4.2$, which was closer to the theoretically predicted value. The simulations for stable inward spiral wave and spiral wave breakup in Eq. (1) are also shown in Fig. 6 for the case of $\varepsilon=1.98$.

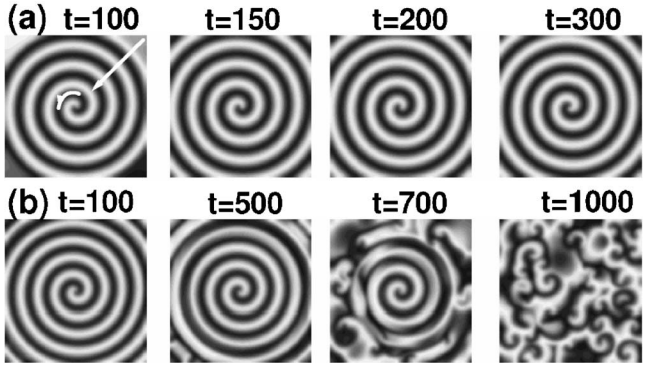

FIG. 5. The snapshots of Re(W) for the inwardly rotating spiral wave at different times in the CGLE of Eq. (2) for various β and $\alpha=-1$. The black to white gray scale represents the lowest value (−1.0) to the highest value (1.0). The arrows indicate the direction of the wave propagation. (a) $\beta=0.3$; (b) $\beta=0.6$. The inwardly spiral wave was stable in (a) while the initiated spiral broke up into a turbulencelike state in (b).

IV. CONCLUSION

We investigated inwardly rotating spiral wave breakup in an oscillatory medium—the FHN model near the supercritical bifurcation point. By increasing the diffusion ratio of the two components of the FHN model, the inwardly rotating spiral arm first broke into a turbulencelike state far away from the core center, which then invaded the whole medium. The same type of wave train breakup was also found in the 1D simulation with one-side fixed or Dirichlet boundary conditions. With the CGLE approximation, we theoretically analyzed the occurrence of the inwardly rotating spiral.

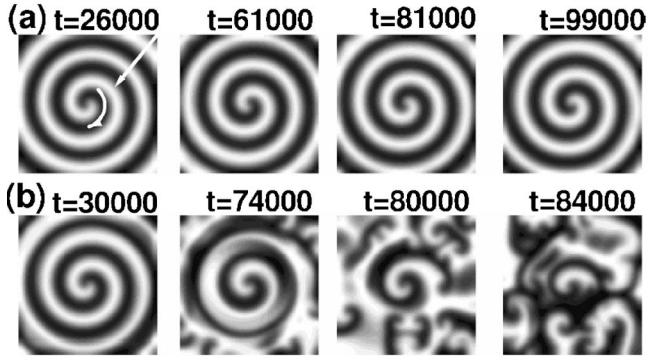

FIG. 6. The snapshots of u for the inwardly rotating spiral wave at different times in the FHN of Eq. (1) for two different γ and $\varepsilon=1.98$. The arrows indicate the direction of wave propagation. (a) $\gamma=4.0$; (b) $\gamma=4.3$. The inwardly spiral wave was stable in (a) while the initiated spiral broke up into multiple spiral waves in (b).

Theoretical analysis of the Eckhaus instability in the CGLE revealed that the breakup of the inwardly rotating spiral wave was related to the Eckhaus absolute instability. The theoretical prediction based on the CGLE approximation agreed reasonably well with the values obtained from numerical simulations in the original oscillatory FHN model near the Hopf bifurcation point. In our theoretical model, the inward spiral wave breakup was controlled by the increasing diffusion ratio of the components in the system. The same strategy could also be applied to the experiments such as the oscillatory BZ-AOT system [2] to test our findings. In addition to the diffusion ratio, the spiral wave breakup could also be controlled by other parameters, such as the droplet fractions ϕ_d and ϕ_{cr} in the oscillatory BZ-AOT system [2]. However, regardless of which control parameters are manipulated, inward spiral wave breakup requires the onset of the Eckhaus absolute instability. Thus, our findings, as well as previous simulation studies [7–11], suggest that spiral wave breakup in a generally oscillatory medium is most likely due to the Eckhaus instability (absolute), regardless of whether the direction of the propagation of the spiral wave is inward or outward.

[1] A. T. Winfree, *When Time Breaks Down* (Princeton University Press, Princeton, 1987); *Chemical Waves and Patterns*, edited by R. Kapral and K. Showalter (Kluwer, Dordrecht, 1995); J. Murray, *Mathematical Biology* (Springer, Berlin, 1989).

[2] V. K. Vanag and I. R. Epstein, Science **294**, 835 (2001).

[3] V. K. Vanag and I. R. Epstein, Phys. Rev. Lett. **87**, 228301 (2001); **88**, 088303 (2002).

[4] Y. F. Gong and D. J. Christini, Phys. Rev. Lett. **90**, 088302 (2003).

[5] L. Brusch, E. M. Nicola, and M. Bär, Phys. Rev. Lett. **92**, 089801 (2004).

[6] E. M. Nicola, L. Brusch, and M. Bär (unpublished).

[7] Q. Ouyang, H. L. Swinney, and G. Li, Phys. Rev. Lett. **84**, 1047 (2000).

[8] M. Bär, M. Hildebrand, M. Eiswirth, M. Falcke, H. Engel, and M. Neufeld, Chaos **4**, 499 (1994).

[9] S. M. Tobias and E. Knobloch, Phys. Rev. Lett. **80**, 4811 (1998).

[10] M. Bär and M. Or-Guil, Phys. Rev. Lett. **82**, 1160 (1999).

[11] B. Sandstede and A. Scheel, Phys. Rev. E **62**, 7708 (2000).

[12] I. S. Aranson, L. Aranson, L. Kramer, and A. Weber, Phys. Rev. A **46**, R2992 (1992).

[13] M. Ipsen, L. Kramer, and P. G. Sorensen, Phys. Rep. **337**, 193 (2000).

[14] I. S. Aranson and K. Kramer, Rev. Mod. Phys. **74**, 99 (2002).

[15] Q. Ouyang and J. M. Flesselles, Nature (London) **379**, 143 (1996).

[16] F. H. Fenton and E. M. Cherry, Chaos **12**, 852 (2002).

[17] J. N. Weiss, H. S. Karagueuzian, Z. L. Qu, and P. S. Chen, Circulation **99**, 2819 (1999).

[18] R. A. FitzHugh, Biophys. J. **1**, 445 (1961).

[19] A. M. Turing, Philos. Trans. R. Soc. London, Ser. B **237**, 37 (1952).

[20] M. C. Cross and P. C. Hohenberg, Rev. Mod. Phys. **65**, 851 (1993), and references therein.

[21] See EPAPS Document No. E-PLEEE8-74-066608 for computer simulation movies. For more information on EPAPS see http://www.aip.org/pubservs/epaps.html.

[22] *Chemical Oscillations, Waves, and Turbulence*, edited by Y. Kuramoto (Springer-Verlag, Berlin, 1984).

[23] P. S. Hagan. SIAM J. Appl. Math. **42**, 762 (1982).